Material-dependent high-frequency current fluctuations of cathodic vacuum arcs: Evidence for the ecton cutoff of the fractal model

André Anders[a)]

Lawrence Berkeley National Laboratory, 1 Cyclotron Road, Berkeley, California 94720

Efim Oks

High Current Electronics Institute, Russian Academy of Sciences, 2/3 Academicheskyi Ave., Tomsk 634055, Russia

ABSTRACT

Current fluctuations of cathodic arcs were recorded with high analog bandwidth (up to 1 GHz) and fast digital sampling (up to 5 Gsamples/sec). The power spectral density of the arc current was determined by fast Fourier transform clearly showing material dependent, non-linear features in the frequency domain. These features can be associated with the non-linear impedance of the conducting channel between cathode and anode, driven by the explosive nature of electron emission and plasma formation. The characteristic times of less than 100 ns can be associated with individual explosive processes, "ectons," and therefore represent the short-time physical cutoff for the fractal model of cathodic arcs.

PACS number: 52.80.Vp

[a)] electronic address: aanders@lbl.gov

I. INTRODUCTION

The emission of electrons from the surface of vacuum arcs cathodes is facilitated by highly non-stationary, non-uniform, and non-linear processes at cathode spots[1]. Electron emission is intimately related to the formation of plasma of the cathode material via explosive destruction of the electron emission center[2]. Although the mechanisms of these processes have been studied for many decades, numerous questions remain unanswered. Looking at the large body of literature on cathode spots one can come to the conclusion that the results obtained by the various experimentalist depended on the equipment used. The greater the time and spatial resolution, the faster processes and smaller structures have been identified. Self-similarity is evident with respect to many physical parameters, which suggests interpreting cathode spot phenomena in the framework of a fractal model[3]. Self-similar, power-law behavior has been found for several cathodic arc phenomena, among them are the size distribution of arc-spot-produced macroparticles [3], the fluctuations of the emitted light[4,5], the ion current in the expanding plasma[4], and the arc burning voltage[6,7].

This work is motivated by further exploring the fractal description of cathodic arcs and identifying possible physical cutoffs at short time and length scales. We should recall that mathematical fractal models are generally defined such that self-similarity exists without limits, i.e. at arbitrarily large or small scales, whereas physical fractals always have cutoffs, e.g. at the small scale when quantum effects appear and at the large scale when the object reaches system dimensions. In the case of cathodic arc spot phenomena, fractal behavior is thought to have physical cutoffs in both the spatial and time domains, which is associated with the elementary processes of electron emission and

plasma production at the small scale and with the cathode size and transient times at the large scale.

Although evidence of elementary processes in the sense of microexplosions has been found, there is no clear picture on the physical cutoffs on the fast temporal and the small spatial scales because ever-improved methods of higher resolution have led to the identification of faster processes and smaller structures. In this contribution, we explore the fractal cutoff on the fast time scale, should it exist within the limits of our enhanced resolution, by investigating the arc *current* fluctuations. As we will show, the results indicate deviations from power laws at high frequencies, which – at least in part – can be interpreted as "fingerprints" of arc processes because they are shown to be material dependent.

Until now, the fluctuations of the arc current have not been considered in fractal research because the arc current is considered to be one of the "smoothest" among arc parameters. This is due to the relatively large impedance that can usually be found in arc discharge circuits, which dampens fluctuations. Therefore, it may appear counterintuitive to consider fluctuations of current as a source of information on fast cathodic arc phenomena. However, spot and arc plasma phenomena are non-linear and therefore might cause non-linear small amplitude current signatures that can be detected by modern equipment.

In the literature, the most clearly postulated cutoff for a fractal model are individual microexplosions that produce bursts of electrons and plasma of the cathode material ("explosive electron emission"[8,9]). Microscopic craters on the cathode surface are evidence for such microexplosions. Based on the theory of wire explosions, it was

postulated that the bursts of explosive release of electrons and plasma cannot be arbitrarily small but need to exceed a critical amount, which Mesyats called "ecton"[2]. In this concept, ectons represent the fast and small-scale cutoffs for a fractal model. In the following, an experimental approach is described for exploring the limits of the fractal model by determining the current fluctuations that cannot be described by a power law, i.e. the high-frequency limits for self-similar behavior.

II. EXPERIMENTAL SETUP AND MEASUREMENTS

A short coaxial cathodic arc plasma source was flange-mounted to a cryogenically pumped vacuum chamber (it was similar to the one described in our previous work on fractal arc voltage[6]). Most experiments were done with a planar anode (as shown in Fig. 1) but some were repeated with an annular anode, which affects the length and position of the conducting channel. For the annular anode geometry, the anode plate was removed and the coaxial tube extended. The tube ended 12 mm beyond the cathode surface plane and therefore there was plenty of anode area in line-of-sight from the cathode surface. Such geometry is similar to our cathodic arc "miniguns"[10].

All experiments were done at the vacuum base pressure, which was about 10^{-4} Pa. Because many single-shot data acquisitions were required, it was appropriate to utilize repetitively pulsed arc discharges. The power supply system was a simple RC discharge with C = 100 μF, charged up to 500 V, switched by a thyristor. In most cases, the current limiting resistor was a 1 Ω ohmic (low-inductance) resistor, but 3 Ω or 0.3 Ω were also used when lower or higher currents were of interest. A second series resistor, a low-inductance shunt of 8.33 mΩ, was used to obtain a current signal proportional to the

current. Data were recorded with carefully selected delay with respect to arc initiation. In the tail of the RC discharge, the current was practically constant during the data acquisition time.

Arc initiation was accomplished by producing a hot spot at the interface between the cathode and a metallized ceramic whose conducting surface was in contact with the anode ("triggerless" or "self-trigger" method[11]). The ceramic tube shielded all but the front face of the 6.25 mm diameter cathode rod, and therefore cathode spots could only burn on the front face of the rod. Due to the erosion (cleaning) action of the spots on the limited cathode area and the intentional delay of data acquisition with respect to arc initiation, arc spots are of type II, i.e. those characteristic for clean, metallic surfaces. Most experiments were done with a flat anode plate positioned 3 mm from the cathode, and some were done with an annular cylinder of 20 mm inner diameter extending 12 mm beyond the cathode plane (i.e., the end of the cathode rod).

Burning voltage and arc current were recorded with very high time resolution using a fast digital oscilloscope. First we used a Tektronix® TDS 744, having 500 MHz analog bandwidth and 2 GS/s sampling rate, and most experiments were repeated with TDS5104B, with 1 GHz analog bandwidth and 5 GS/s sampling rate. The oscilloscope was set to record between 50,000 to 2,000,000 data points for each data acquisition. Most recording was done with 500,000 points because a larger number did not give much more information while unreasonably increasing the computation time, which increases exponentially with the number of data points. When using 500,000 points, the total data acquisition time was 40 μs, with 80 ps between data points.

First, a somewhat longer cathode rod was used such that the cathode was in contact with the planar disk anode, thereby creating an electric short. This enabled us to record data without creating an arc. These data represent the "zero line" from which we may distinguish arc-related frequency phenomena, should they exist. Figures 2 and 3 show the no-arc "zero-line," which exhibits a $1/f^2$ slope due to the inductance of the circuits (discussed later). When the cathode was retracted such that a discharge gap of 3 mm was formed, cathodic arcs could burn and the procedure was repeated. Depending on the cathode material, one obtained more or less strong peaks in the frequency region between 10^7 and 10^9 Hz. (Figs. 2 and 3).

When using the coaxial geometry, the same features were observed with slightly greater peak amplitude. The slightly greater peaks are likely related to the greater circuit inductance which includes the longer current-carrying plasma channel. Because we are mostly interested in cathode spot processes, all results shown here were done with the planar anode geometry shown in Fig. 1.

To check whether the features seen are peculiar to tungsten, the cathode was replaced by tantalum, and the influence of the arc current was systematically studied. The result is shown in Fig. 4. As with tungsten, various peaks appeared in the region 10-300 MHz. Interestingly, the distribution of the power spectral density (PSD) for Ta was different than the PSD for W. As the current was reduced, the general shape of the PSD was maintained but the values were increased and the onset of non-power-law behavior occurred at lower frequencies.

The series of measurements was extended to other cathode materials, including carbon, magnesium, and nickel. The data for 20 A arc current are shown in Fig. 5.

Nickel exhibited strong fluctuations which extended all the way down to 40 MHz. In contrast, Mg and C cathodes appeared to operate relatively "smoothly."

III. DATA PROCESSING

The single-pulse data were exported from the digital oscilloscope to a computer for Fourier transform analysis. Because the time-domain data are arrays of discrete data points rather than continuous functions, discrete Fourier transform (DFT) needed to be applied. The inverse of the sampling period represents a lower limit to the (digital) resolution of the transformed data (25 kHz). The upper limit is given by one half of the inverse of the sampling interval (Nyquist sampling theorem), which is 6.25 GHz. Obviously, digital effects limit the resolution at low frequency (the DFT curves exhibit unphysical oscillations) while the analog bandwidth represents the true upper resolution limit (1 GHz).

Conventionally, DFT is executed by fast algorithms that utilize certain symmetries in the data set (fast Fourier transform, FFT). We used the Danielson-Lanczos algorithm as implemented in Origin® software. Each measurement was repeated 10 times (while keeping discharge conditions constant), and FFT was applied to each data set individually. The sets of FFT data for constant conditions were averaged to reduce the noise in the frequency domain. It is should be stressed that the averaging procedure was applied *after* FFT, otherwise one would have lost valuable information that might be contained in the fluctuations of the signal in the time domain.

IV. DISCUSSION

According to the ecton and similar models, each microexplosion facilitates the emission of a limited charge, whose average value shall be denoted by $\langle \delta Q \rangle = \left\langle \int_0^{\delta t} \delta I \, dt \right\rangle$, where the brackets $\langle \ \rangle$ indicate averaging over a large number of emission events; δt indicates the duration of the emissive phase of a spot cell (also known as "lifetime"). Within the ecton or similar explosive emission concepts, the lifetime is thought to be in the nanosecond range based on modeling [12,13] and optical experiments with very high temporal resolution [14,15]. However, longer "characteristic times" have been seen in optical emission[16], too, which have led to the formulation of self-consistent models for the cathodic arc spot not based on the ecton concept. In such models, strong evaporation and ionization of vapor in some distance from he solid cathode surface is assumed[17]. The fractal model, on the other hand, allows us to reconcile these apparently contradicting descriptions by accepting explosive events as a limit (cutoff of self-similarity at short times and length scale) and the existence of areas with evaporation and ionization in parallel with the explosive events. Evaporation and ionization are slower and larger scale processes containing self-similar dynamic patterns, i.e. the self-similarity applies to temporal and spatial dimensions.

To carry the arc current, several emission events (cells) are active at any given time,

$$\langle N_{cells} \rangle = \frac{I_{arc}}{\langle \delta Q / \delta t \rangle}. \tag{1}$$

The number of simultaneously active cells is not known and is certainly a fluctuating value related to the noise of the discharge current. According to Eq. (1), reducing the arc current would reduce the number of active cells and thereby increasing

the level of noise because each the ignition and decay of each cell has a greater weight in contributing to the production of charge carriers. Fig. 3 showed the result obtained under the same conditions as with Fig. 2 but at 20 A (instead of 100 A). We see that the general character of the noise is maintained but the peaks are more pronounced, with some additional peaks appearing at lower frequency. These features are expected in the ecton or similar models because the fluctuations seen represent the composite of many events occurring at the level of self-similarity cutoff. The greater the current and the number of individual emission events, the smaller the relative contribution of each individual emission event, and therefore the current signal appears smoother. The noise at lower frequency appears greater because the "gaps" between emission events at lower current are longer.

To further interpret these measurements, one may consider the equivalent circuit consisting of the following series elements: the voltage source (the 100 μF capacitor), V_0, the main resistor, R, an inductance due to cables, L, the shunt resistance, R_{shunt}, and the complex impedance of the arc, $\mathbf{Z}_{arc}$, which consists of two parallel branches, one with arc resistance and inductance in series and the other being a capacitance. Then, the phasor current is according to Ohm's law

$$\mathbf{I} = \frac{\mathbf{V}}{\mathbf{Z}} = \frac{\mathbf{V}}{R + \mathbf{Z}_L + R_{shunt} + \mathbf{Z}_{arc}}, \tag{2}$$

where the bold font indicates (complex) phasors[18]. In a first approximation, $\left|\mathbf{Z}_{arc}\right| \ll \left|R + R_{shunt} + \mathbf{Z}_L\right|$, and one can realize that this circuit represents a first order low pass filter for a voltage measured at R_{shunt}. Using the fact that all time-dependent signals

can be composed as a sum over their Fourier components with angular frequency $\omega = 2\pi f$, one can express the measured voltage V_{shunt} via the transfer function

$$H(f) = \frac{\mathbf{V_{shunt}}}{\mathbf{V_0}} = \frac{1}{1 + i(f / f_B)} \tag{3}$$

where f_B is the half power frequency

$$f_B = (R + R_{shunt}) / 2\pi L \tag{4}$$

and $i = \sqrt{-1}$. For our experimental conditions, $f_B \sim 10 - 100$ kHz, which is below the lower limit of resolution. For frequencies higher than f_B, the Bode plot (transfer function in decibels versus logarithmic frequency) shows –20 dB per decade or –3 dB per octave. For the power spectral density, we have to take the square of the transfer function and find $|H(f)|^2 = 1/(1 + (f / f_B))^2$, which reproduces the $1/f^2$ dependence seen in the experiment. Therefore, the slope of the current PSD is not associated with fractal behavior but due to circuit inductance which dampens fluctuations proportional to $1/f$ when considering the spectral amplitude, and $1/f^2$ when considering the spectral power.

In the linear theory, there is no way to derive expressions that would lead to the peaks seen in the PSD. The transfer function cannot be described by simple expressions like (3) and (4) but one should expect highly non-linear behavior.

The frequency interval where deviation from the $1/f^2$ behavior occurs allows us to draw some conclusions on the timescale of non-linear circuit behavior and the cathode processes affecting it.

The plasma formed in a microexplosion expands from the emission center, filling the gap between cathode and anode. This represents the formation and decay of a

conducting channel. The inductance is determined by the effective diameter and length of the plasma channel, which are variables, hence L_{arc} is a function of time.

The cathode sheath behaves like a capacitor, accommodating the voltage difference between plasma potential and cathode potential. The sheath thickness is a function of the local plasma density (self-adjusting Debye sheath), which in turn is a function of the non-stationary plasma production and distance from the plasma emission center. Both the arc inductance and arc capacitance are related to the same plasma production and expansion processes. Their characteristic times are related to the duration of the emission events (lifetime of emission center or spot cell), the time between ignition of emission centers, and the transit time of plasma bridging the cathode-anode gap. The latter is most easily estimated based on measured ion velocities[19], giving us values between 100 ns and 1 μs, depending on cathode material. The other times are expected to be shorter[14,15] and fall within the observed frequency interval of non-$1/f^2$ current noise.

To further evaluate the relevance of the two branches of the equivalent circuit for the arc, one may estimate reasonable characteristic values in $i\omega L_{arc}(t)$ and $1/\left(i\omega C_{arc}(t)\right)$, which leads to the finding that the impedance of the capacitive branch is much higher than the impedance of the inductive branch. This is consistent with the observation that the shape and position of the peaks in the PSD are slightly modified when the anode size and position is changed. One can conclude that although the material-dependent PSD curves are triggered and stimulated by fast cathode processes, and therefore contain information on these processes, they are also related to the entire arc circuit, which complicates interpretation.

In particular, one may ask the question on the relation of current fluctuations and voltage fluctuations. The peaks observed in the current PSD suggest that similar peaks might exist in the voltage PSD. Indeed, we have previously reported on such peaks in some of the voltage PSD[6] without being able to conclusively ascribe them to elementary emission processes. The results presented here suggest further evidence for such interpretation but ultimately one would need to eliminate circuit effects to conclusively make the case. In any case, the experimental result show that there is no linear relationship between voltage and current, rather, peaks in the current PSD and voltage PSD, if they exist, are not exactly at the same frequency.

V. CONCLUSIONS

In conclusion, we have observed that fluctuations of the cathodic arc current exhibits material dependent non-linear effects for time scales of about 10 ns and shorter, which can be associated with fast changes of the arc inductance. These changes are related to fast cathode processes, i.e. the formation of decay of conducting channel between cathode and anode. However, the power spectral density is determined by all factors affecting the circuit impedance, such as the position of the anode. The observed peaks in the power spectral density in the frequency domain correspond to times of order 10 ns, which is consistent with characteristic times in the ecton model. These finding provide some evidence that the fractal model of cathode spots has a physical cutoff at short times of less than 100 ns, the specific values being dependent on the material and current level. Further research needs to focus on eliminating circuit effects that influence peaks in the PSD.

ACKNOWLEDGEMENTS

E.O. acknowledges support by the Russian Foundation for Basic Research under the Grant # 02-05-16256-a. This work was supported by the U.S. Department of Energy, Initiatives for Proliferation Prevention, Project No. IPP-LBNL-T2-196, under Contract No. DE-AC02-05CH11231 with the Lawrence Berkeley National Laboratory.

Figure Captions

Fig. 1 Coaxial plasma source shown here with the planar anode. The electrical connections to power supply and shunt are schematically shown. For dimensions: the cathode rod had a diameter of 6.25 mm.

Fig. 2 Power spectral density of current fluctuations, obtained by FFT of the shunt signal when current is driven through a short (anode and cathode in contact, lower curve) and when a cathodic arc burns on a tungsten cathode (upper curve). The current was 100 A in both cases. For better display, the short-circuit data were divided by 10, shifting the curve down. The band of regular oscillations, visible at the low frequency end, is an artifact of the discrete Fourier transform. The short-circuit curve exhibits a narrow peak at 10^8 Hz indicating a circuit resonance.

Fig. 3 Power spectral density as in Fig. 2 but measured at 20 A arc current.

Fig. 4 Power spectral density for tantalum arcs at different arc currents.

Fig. 5 Power spectral density for nickel, magnesium, and carbon arcs, measured at a discharge current of 20 A.

References

[1] B. Jüttner, J. Phys. D: Appl. Phys. **34,** R103-R123 (2001).

[2] G. A. Mesyats, IEEE Trans. Plasma Sci. **23,** 879-883 (1995).

[3] A. Anders, IEEE Trans. Plasma Sci. **33,** 1456-1464 (2005).

[4] R. P. P. Smeets and F. J. H. Schulpen, J. Phys. D: Appl. Phys. **21,** 301-310 (1988).

[5] T. Schülke and P. Siemroth, IEEE Trans. Plasma Sci. **24,** 63-64 (1996).

[6] A. Anders, E. M. Oks, and G. Yu.Yushkov, Appl. Phys. Lett. **86,** 211503-1-3 (2005).

[7] J. Rosén and A. Anders, J. Phys. D: Appl. Phys. **38,** 4184-4190 (2005).

[8] S. P. Bugaev, E. A. Litvinov, G. A. Mesyats, and D. I. Proskurovskii, Sov. Phys. Usp. **18,** 51-61 (1975).

[9] G. A. Mesyats, *Explosive Electron Emission* (URO Press, Ekaterinburg, 1998).

[10] R. A. MacGill, M. R. Dickinson, A. Anders, O. R. Monteiro, and I. G. Brown, Rev. Sci. Instrum. **69,** 801-803 (1998).

[11] A. Anders, I. G. Brown, R. A. MacGill, and M. R. Dickinson, J. Phys. D: Appl. Phys. **31,** 584-587 (1998).

[12] S. A. Barengolts, G. A. Mesyats, and D. L. Shmelev, IEEE Trans. Plasma Sci. **31,** 809-816 (2003).

[13] I. V. Uimanov, IEEE Trans. Plasma Sci. **31,** 822-826 (2003).

[14] A. Anders, S. Anders, B. Jüttner, W. Bötticher, H. Lück, and G. Schröder, IEEE Trans. Plasma Sci. **20,** 466-472 (1992).

[15] B. Jüttner, IEEE Trans. Plasma Sci. **27,** 836-844 (1999).

[16] I. Beilis, B. E. Djakov, B. Jüttner, and H. Pursch, J. Phys. D: Appl. Phys **30,** 119-130 (1997).

[17] I. I. Beilis, Appl. Phys. Lett. **84,** 1269-1271 (2004).

[18] A. R. Hambley, *Elecrical Engineering: Principles and Applications*, 2nd ed. (Prentice Hall, Upper Saddle River, NJ, 2002).

[19] A. Anders and G. Y. Yushkov, J. Appl. Phys. **91,** 4824-4832 (2002).

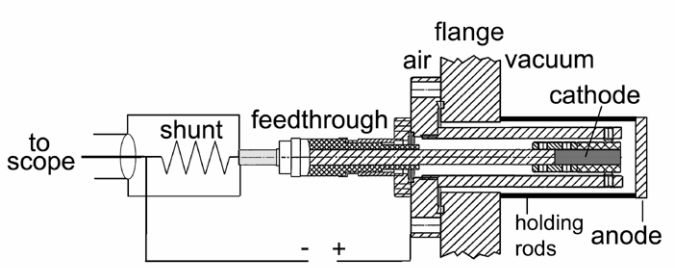
flange
air
vacuum
cathode
shunt
feedthrough
to
scope
holding
rods
anode
-
+

Fig. 1

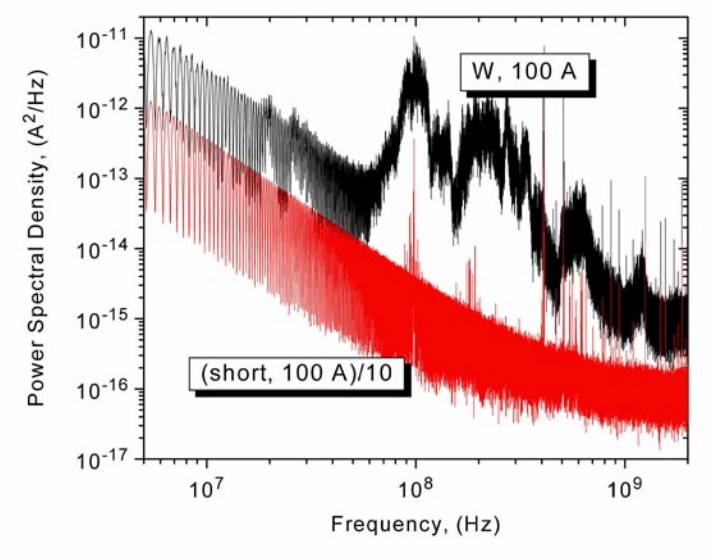
Power Spectral Density, (A²/Hz)
10⁻¹¹
10⁻¹²
10⁻¹³
10⁻¹⁴
10⁻¹⁵
10⁻¹⁶
10⁻¹⁷
10⁷
10⁸
10⁹
Frequency, (Hz)
W, 100 A
(short, 100 A)/10

Fig. 2

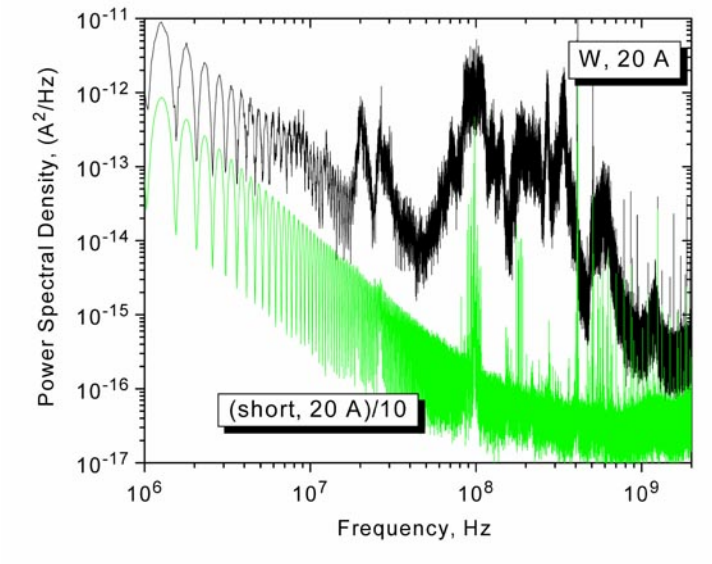
Power Spectral Density, (A²/Hz)
Frequency, Hz
W, 20 A
(short, 20 A)/10
10⁻¹¹
10⁻¹²
10⁻¹³
10⁻¹⁴
10⁻¹⁵
10⁻¹⁶
10⁻¹⁷
10⁶
10⁷
10⁸
10⁹

Fig. 3

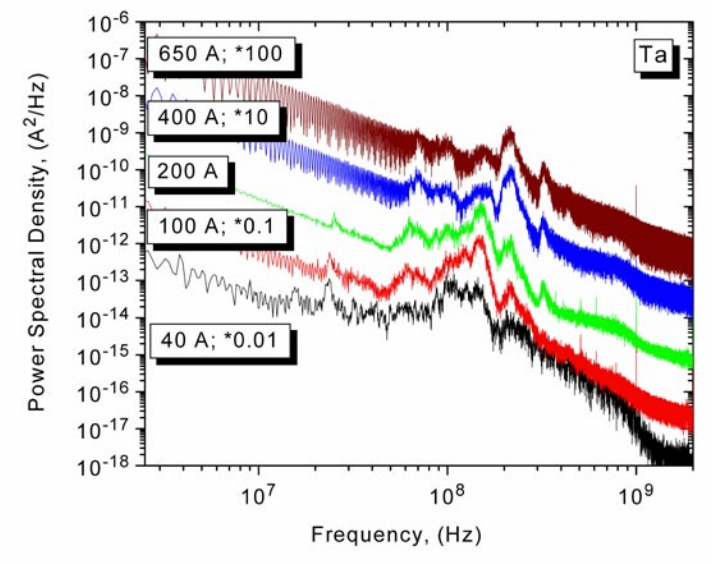
650 A; *100
400 A; *10
200 A
100 A; *0.1
40 A; *0.01
Ta
Power Spectral Density, (A²/Hz)
Frequency, (Hz)
10⁻⁶
10⁻⁷
10⁻⁸
10⁻⁹
10⁻¹⁰
10⁻¹¹
10⁻¹²
10⁻¹³
10⁻¹⁴
10⁻¹⁵
10⁻¹⁶
10⁻¹⁷
10⁻¹⁸
10⁷
10⁸
10⁹

Fig. 4

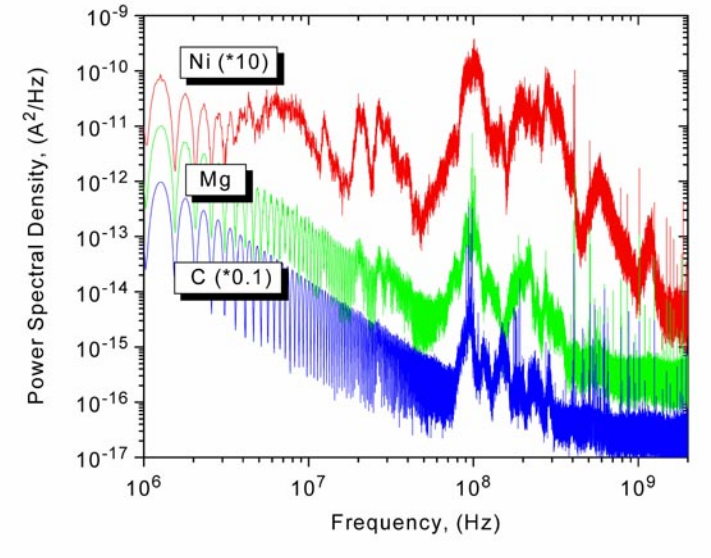
Ni (*10)
Mg
C (*0.1)
Power Spectral Density, (A²/Hz)
Frequency, (Hz)
10⁻⁹
10⁻¹⁰
10⁻¹¹
10⁻¹²
10⁻¹³
10⁻¹⁴
10⁻¹⁵
10⁻¹⁶
10⁻¹⁷
10⁶
10⁷
10⁸
10⁹

Fig. 5